Nuclear Magnetic Shielding and Aromaticity of [18]Annulene and Its Quasi-Möbius-Type Analogues

Hirotaka Tanimura, Yasushi Honda, Ken-ichi Sugiura, and Masahiko Hada*

Department of Chemistry, Graduate School of Science and Engineering, Tokyo Metropolitan University, 1-1 Minami-Osawa, Hachioji, Tokyo 192-0397

Received September 7, 2010; E-mail: hada@tmu.ac.jp

We presented a series of quantum-chemical calculations of [18]annulene ($C_{18}H_{18}$) and its analogues which are helically distorted open-chain molecules and which we call "*quasi-Möbius-type*" molecules in this paper. We discussed the proton magnetic shielding constants, the chemical shifts, and the nucleus-independent chemical shift (NICS) of these molecules. The calculated nuclear magnetic shielding constants were decomposed into the diamagnetic and paramagnetic terms using a conventional manner. As we expected, a shielding–deshielding reversal occurs in $C_{18}H_{18}$ and quasi-Möbius-type $C_{18}H_{20}$. Moreover, we showed a predictive demonstration that the magnetic shielding constants can be controlled by inserting a small molecule such as CH_3^- or $H_2C{=}CH_2$ into the terminal π-orbitals of quasi-Möbius-type $C_{18}H_{20}$ or $C_{16}H_{18}$. Aromaticity and antiaromaticity are discussed with magnetic features of molecules.

Aromaticity is a chemical characteristic of π-electron systems related to π-electron configurations and stabilities, molecular structures, magnetic properties, chemical reactivity, and so on. The concept of aromaticity has been modified gradually and greatly so far[1] and so its definition has been not yet completely established. In aromatic systems, substitution reactions occur more easily than addition reactions.[2] The heat of combustion is lower than other unsaturated molecules.[3] According to the well-known Hückel rule, $(4n + 2)\pi$-electron systems are defined as an aromatic system. As an accompanying concept, $4n\pi$-electron systems are defined as an antiaromatic system,[4–6] though the chemical definition of antiaromaticity is somewhat unclear. In the well-known Möbius-type π-electron systems, $4n\pi$-electron systems are aromatic, and this rule is called Möbius aromaticity.[7–9] The Möbius aromaticity had been predicted theoretically.[10–12] It was confirmed experimentally[13–18] in the 21st century, and further theoretical studies have been reported.[18–24] Recent research on Möbius-type molecules is summarized in Ref. 9.

Some magnetic properties of cyclic π-electron systems conventionally have been explained with the ring current model (RCM). The concept of a ring current appeared in the 1960s with benzene and [18]annulene as typical examples.[25–28] In aromatic compounds, an external magnetic field generates a ring current, and then it generates an induced magnetic field, the direction of which is opposite to the applied external magnetic field inside the ring. Therefore the inside of the ring is magnetically shielded and the outside is deshielded. This is called the Pople model.[29–31] It is well known that this phenomenon changes by the number of π-electrons. Heine et al.[21] recently carried out an accurate quantum chemical calculation and theoretically suggested the existence of the ring current. Taubert et al.[23,24] investigated magnetically induced current density on various aromatic and antiaromatic molecules. However, the ring current is a theoretical concept and it is not substantial.[32]

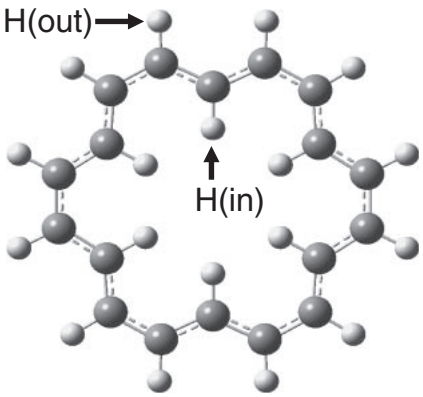

Figure 1. [18]Annulene ($C_{18}H_{18}$) and two resonance protons calculated.

In 1996, Schleyer et al. presented a useful index for aromaticity which is called the nucleus-independent chemical shift (NICS).[33] If the NICS is negatively large at the center of a π-ring system, it is defined as aromatic. On the contrary, if the NICS is positive, it is formally defined as antiaromatic. Recently the NICS is frequently used by organic chemists.[34]

In this study, we treated [18]annulene shown in Figure 1 and its hypothetical analogues. Sondheimer reported a first synthesis of [18]annulene in 1962.[35] [18]Annulene is a completely conjugated monocyclic hydrocarbon which contains 18 carbons and 18π-electrons. In 1965, Weiss, Jr. et al. carried out the first ab initio calculation of [18]annulene.[36] Thereafter, there have been many computational studies of [18]annulene.[37–39]

We carried out a series of ab initio quantum-chemical MO calculations of [18]annulene and its analogues including helically distorted $C_{18}H_{20}$ which we call a *quasi-Möbius-type*

Published on the web July 30, 2011; doi:10.1246/bcsj.20100257

molecule shown in Figure 7. The reason why we call this molecule quasi-Möbius-type will be given in the section of Results and Discussion. Then, we calculated the ^{1}H magnetic shielding constants, the ^{1}H NMR chemical shifts, and the NICS of these molecules. We also studied aromaticity and antiaromaticity from the viewpoint of magnetic properties.

Method

Nuclear magnetic shielding tensor σ_{Ntu} $(t, u = x, y, z)$ is expressed as a second-order derivative of the total energy E which is called Ramsey's formula,[40–43]

$$\sigma_{Ntu} = \left.\frac{\partial^2 E}{\partial \mu_{Nt} \partial B_{0u}}\right|_{B_0=\mu_N=0} \quad (t, u = x, y, z) \tag{1}$$

where μ_N is the nuclear magnetic moment of nucleus N and B_0 is the external uniform magnetic field. We briefly review a decomposition of the nuclear magnetic shielding tensor for the present report. The magnetic shielding tensor is decomposed into two contributions[44,45] as

$$\sigma_{Ntu} = \sigma(dia)_{Ntu} + \sigma(para)_{Ntu} \quad (t, u = x, y, z) \tag{2}$$

The $\sigma(dia)_{Ntu}$ and $\sigma(para)_{Ntu}$ in eq 2 are called the diamagnetic and the paramagnetic shielding tensors, respectively. In the second-order perturbation theory and in the framework of the nonrelativistic theory, $\sigma(dia)_{Ntu}$ is expressed as

$$\begin{aligned}\sigma(dia)_{Ntu} &= \frac{e^2\mu_0}{4m_e}\langle 0|\frac{\mathbf{r}\cdot\mathbf{r}_N\delta_{tu} - r_t r_{Nu}}{{r_N}^3}|0\rangle \\ &= \frac{e^2\mu_0}{4m_e}\int \rho(\mathbf{r})\frac{\mathbf{r}\cdot\mathbf{r}_N\delta_{tu} - r_t r_{Nu}}{{r_N}^3}\,\mathrm{d}\mathbf{r}\end{aligned} \tag{3}$$

μ_0 is the permeability of vacuum. The $\sigma(dia)_{Ntu}$ is rewritten by using the position operator $\mathbf{r}$ and the electron density $\rho(\mathbf{r})$. Therefore, the $\sigma(dia)_{Ntu}$ depends on the electron density around the resonance nucleus. The $\sigma(para)_{Ntu}$ is expressed as

$$\sigma(para)_{Ntu} = \frac{e^2\mu_0}{2{m_e}^2}\sum_{m\neq 0}\frac{\langle 0|\hat{L}_t|m\rangle\langle m|\dfrac{\hat{L}_{Nu}}{{r_N}^3}|0\rangle}{E_0 - E_m} \tag{4}$$

$|m\rangle$ is a wave function of an excited state. L_t is the orbital angular momentum of electrons, and L_{Nu} is the angular momentum of electrons around the nucleus N $(t, u = x, y, z)$. Equation 4 is approximately rewritten in the framework of the Hartree–Fock theory as

$$\sigma(para)_{Ntu} \approx \frac{e^2\mu_0}{2{m_e}^2}\sum_{k}^{occ}\sum_{a}^{unocc}\frac{\langle k|\hat{L}_t|a\rangle\langle a|\dfrac{\hat{L}_{Nu}}{{r_N}^3}|k\rangle}{\varepsilon_k - \varepsilon_a} \tag{4'}$$

Because $\sigma(para)_{Ntu}$ includes the angular momentum operator, it usually contributes as a deshielding term by the magnetic response of the angular momentum. In many cases, the magnetic shielding constant changes by various $\sigma(para)_{Ntu}$. According to eq 4, the change of $\sigma(para)_{Ntu}$ depends on the difference between the energy of the ground state and that of the excited state.

Isotropic component $\sigma_{N,iso}$ is an average of xx, yy, and zz components.

$$\sigma_{N,iso} = \frac{\sigma_{Nxx} + \sigma_{Nyy} + \sigma_{Nzz}}{3} \tag{5}$$

The chemical shift δ is defined as

$$\delta_N = \sigma_{N,iso}[ref] - \sigma_{N,iso} \tag{6}$$

where $\sigma_{N,iso}[ref]$ is the isotropic nuclear magnetic shielding constant of a standard molecule. The standard molecule in this study is tetramethylsilane (TMS).

We also calculated the nuclear independent chemical shift (NICS)[33] in the same procedure as calculations of NMR chemical shifts. The resonance point was put in the center of cyclic compounds. In the case of NICS, we replace $\sigma_{N,iso}$ with σ_{iso}. The reference $\sigma_{iso}[ref]$ is taken from the vacuum.

$$\begin{aligned}\mathrm{NICS} &= \sigma_{iso}(vacuum) - \sigma_{iso}(center) \\ &= 0 - \sigma_{iso}(center) \\ &= -\sigma_{iso}(center)\end{aligned} \tag{7}$$

Negative NICS values indicate aromaticity, while positive NICS values indicate antiaromaticity. We generally call the NICS value of the ring center NICS(0). NICS is said to depend on the ring size of cyclic compounds.

In this paper, we treated [18]annulene $C_{18}H_{18}$ (18π-electrons), $C_{18}H_{18}{}^{2-}$ (20π-electrons), and open-chain $C_{16}H_{18}$ (16π-electrons) made by removing two carbons from $C_{18}H_{18}$. We also treated the quasi-Möbius-type open-chain $C_{18}H_{20}$ (18π-electrons). Finally we treated $C_{18}H_{20} + CH_3{}^-$ (20π-electrons) and $C_{16}H_{18} + H_2C{=}CH_2$ (18π-electrons). Since all these molecules are in the singlet state, ^{1}H magnetic shielding constants were calculated by the restricted Hartree–Fock (RHF) method and/or the restricted B3LYP (RB3LYP) method. We used 6-311G(d,p) as basis sets. The geometry optimization method we employed was B3LYP/6-311G(d,p). Molecular structures of $C_{18}H_{18}$ and $C_{18}H_{18}{}^{2-}$ were optimized by this method. The optimization procedures for the other systems will be given later. In calculations of ^{1}H magnetic shielding constants, the magnetic field was treated by the gauge-independent atomic orbital (GIAO) method.[25,46] All calculations were performed by Gaussian 03 program.[47]

Results and Discussion

Accuracy Check. Table 1 shows the proton NMR chemical shifts of various cyclic π-conjugated molecules, which are measured[48] and calculated by the RHF and DFT (B3LYP) methods. The symbols (A)–(D) indicate nonequivalent protons in a molecule. The agreement with the chemical shifts calculated and measured is satisfactory for discussions in the following sections. Errors are less than 1.0 ppm except for one molecule in RHF and two molecules in B3LYP. Both methods reproduce the experimental trend sufficiently for the present purpose. We use the RHF method hereafter because in an interpretation and an analysis using the second-order perturbation theory, the molecular orbital (MO) theory may have a clearer meaning than the Kohn–Sham theory. Moreover, in some cases, the B3LYP method cannot describe sufficiently the long-range interactions, e.g., the charge transfer and the van der Waals force.[49] After this, all NMR calculations were carried out by the RHF method, and the molecular geometries of $C_{18}H_{18}$ and $C_{18}H_{18}{}^{2-}$ were determined by the B3LYP method.

Neutral [18]Annulene and Its Double Anion. Figure 2 shows a part of the molecular structure of [18]annulene ($C_{18}H_{18}$) and the geometrical parameters optimized at

Table 1. Calculated and Measured ^{1}H NMR Chemical Shifts of Cyclic π-Conjugated Molecules by RHF/6-311G(d,p) and RB3LYP/6-311G(d,p) (ppm)

Molecule	RHF		B3LYP		δ(exptl)[a)]
	δ(calcd)	error	δ(calcd)	error	
Cyclopropane	0.88	0.68	0.88	0.68	0.20
Cyclobutane	2.57	0.61	2.70	0.74	1.96
Cyclopentane	2.40	0.90	2.61	1.11	1.50
Benzene	7.88	0.54	7.72	0.38	7.34
Cyclopentene (A)	6.10	0.37	6.04	0.31	5.73
Cyclopentene (B)	2.91	0.61	3.20	0.90	2.30
Cyclopentene (C)	2.49	0.67	2.57	0.75	1.82
Cyclopentadiene (A)	6.89	0.46	6.93	0.50	6.43
Cyclopentadiene (B)	6.90	0.62	6.81	0.53	6.28
Cyclopentadiene (C)	3.28	0.48	3.51	0.71	2.80
1,3,5-Cycloheptatriene (A)	6.76	0.18	6.84	0.26	6.58
1,3,5-Cycloheptatriene (B)	6.36	0.18	6.51	0.33	6.18
1,3,5-Cycloheptatriene (C)	5.82	0.46	5.64	0.28	5.36
1,3,5-Cycloheptatriene (D)	3.18	0.94	3.48	1.24	2.24
Pyrrole (A)	7.09	−0.91	7.13	−0.87	8.00
Pyrrole (B)	7.42	0.68	7.07	0.33	6.74
Pyrrole (C)	6.87	0.63	6.72	0.48	6.24
Pyridine (A)	7.64	0.36	7.54	0.26	7.28
Pyridine (B)	8.33	0.67	7.97	0.31	7.66
Pyridine (C)	9.46	0.85	9.26	0.65	8.61
Pyrimidine (A)	10.23	0.96	10.11	0.84	9.27
Pyrimidine (B)	9.63	0.85	9.35	0.57	8.78
Pyrimidine (C)	7.50	0.12	7.45	0.07	7.38
Pyrazine	9.41	0.82	9.16	0.57	8.59
Pyridazine (A)	7.91	0.39	7.56	0.04	7.52
Pyridazine (B)	10.22	1.01	9.94	0.73	9.21

a) Ref. 47.

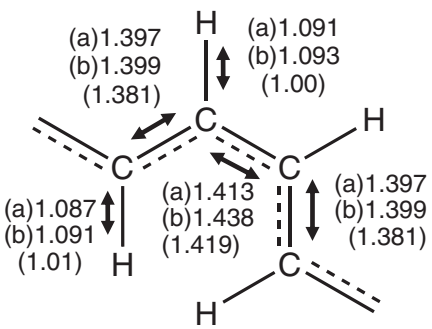

Figure 2. Internuclear distances of [18]annulene ($C_{18}H_{18}$) (a) and [18]annulene dianion ($C_{18}H_{18}^{2-}$) (b), respectively, in Å. Values in parentheses are the corresponding experimental ones of $C_{18}H_{18}$.

RB3LYP/6-311G(d,p) level. Values in parentheses are experimental values of the crystal structure.[50,51] Agreement between calculated and experimental geometric parameters is satisfactory and the bond alternation peculiar to the aromatic compound is also reproduced. We utilized these optimized parameters to calculate the magnetic properties.

Table 2 shows the ^{1}H magnetic shielding constants and chemical shifts of $C_{18}H_{18}$ and $C_{18}H_{18}^{2-}$. The H(out) and H(in) represent the hydrogens outside and inside the $C_{18}H_{18}$ ring, respectively, as shown in Figure 3. The calculated proton chemical shifts generally reproduced the experimental trend. In the neutral [18]annulene, the experimental values of ^{1}H NMR chemical shifts are 9.28 and 2.99 ppm for H(out) and H(in), respectively,[52] while calculated values were 12.05 and −12.56 ppm for H(out) and H(in), respectively. The difference between the experimental and calculated values for the H(in) were relatively large (ca. 15 ppm), in contrast to the relatively well-reproduced H(out). However, the qualitative tendency shows good accordance in terms that the H(out) is deshielded more than the H(in) in $C_{18}H_{18}$, and this result is adequate later discussion. In $C_{18}H_{18}^{2-}$, the experimental values of ^{1}H NMR chemical shifts are −1.10 and 20.8/29.5 ppm for H(out) and H(in), respectively.[53] Since $C_{18}H_{18}^{2-}$ exists in solution as an equilibrium between two species (D_{6h}:D_3 = 7:3),[54] two experimental values were reported for H(in). The corresponding calculated values were 0.80 and 22.60 ppm for H(out) and H(in), respectively. We safely mention that the accuracy of RHF method is sufficient to accomplish the following analyses.

The neutral [18]annulene is a typical aromatic molecules. The outside hydrogens are deshielded and the inside ones are shielded. On the other hand, $C_{18}H_{18}^{2-}$ shows a result contrary to the neutral $C_{18}H_{18}$, namely, the H(out) shows an upfield shift and H(in) a downfield shift, as we expected. $C_{18}H_{18}$ has 18π-electrons and belongs to the $(4n+2)\pi$-electron systems, whereas $C_{18}H_{18}^{2-}$ has 20π-electrons, i.e., a $4n\pi$-electron system. According to the conventional Hückel rule, the former

Table 2. ^{1}H NMR Chemical Shifts of $C_{18}H_{18}$ and $C_{18}H_{18}^{2-}$ by RHF/6-311G(d,p) (ppm)[a]

Molecule	Number of π-electrons	H(out)[b]		H(in)[b]	
		δ(calcd)	δ(exptl)	δ(calcd)	δ(exptl)
[18]Annulene $C_{18}H_{18}$	18	12.05	9.28[c]	−12.56	2.99[c]
[18]Annulene dianion $C_{18}H_{18}^{2-}$	20	0.80	−1.10[d]	22.60	20.8, 29.5[d,e]

a) The reference molecule is TMS. b) See Figure 1. c) Ref. 51. d) Ref. 52. e) Since the dianion exists as an equilibrium between two species (D_{6h}:D_3 = 7:3) in solution,[53] two values are reported.

Table 3. ^{1}H Magnetic Shielding Constants of $C_{18}H_{18}$, $C_{18}H_{18}^{2-}$, $C_{16}H_{18}$, Quasi-Möbius-Type $C_{18}H_{20}$ (R = 1.5, 2.0, and 3.0 Å), Quasi-Möbius-Type $C_{18}H_{20}$ + Methyl Anion, and $C_{16}H_{18}$ + Ethylene (ppm)

Molecule	Number of π-electrons	H(out)			H(in)		
		σ(*dia*)	σ(*para*)	σ(*total*)	σ(*dia*)	σ(*para*)	σ(*total*)
$C_{18}H_{18}$	18	29.71	−9.52	20.19	40.34	4.46	44.80
$C_{18}H_{18}^{2-}$	20	31.32	0.18	31.50	37.34	−27.70	9.64
$C_{16}H_{18}$	16	23.44	2.30	25.74	39.70	−17.07	22.63
$C_{18}H_{20}$ (R = 1.5 Å)[a]	18	22.69	7.13	29.82	38.57	−31.67	6.90
$C_{18}H_{20}$ (R = 2.0 Å)[a]	18	29.38	−1.53	27.85	39.97	−24.52	15.45
$C_{18}H_{20}$ (R = 3.0 Å)[a]	18	29.52	−3.13	26.39	41.17	−20.13	21.04
$C_{18}H_{20} + CH_3^-$	20	28.37	−2.94	25.43	37.90	−7.13	30.77
$C_{16}H_{18} + H_2C{=}CH_2$	18	23.70	0.24	23.94	39.08	−8.98	30.10

a) R is shown in Figure 2.

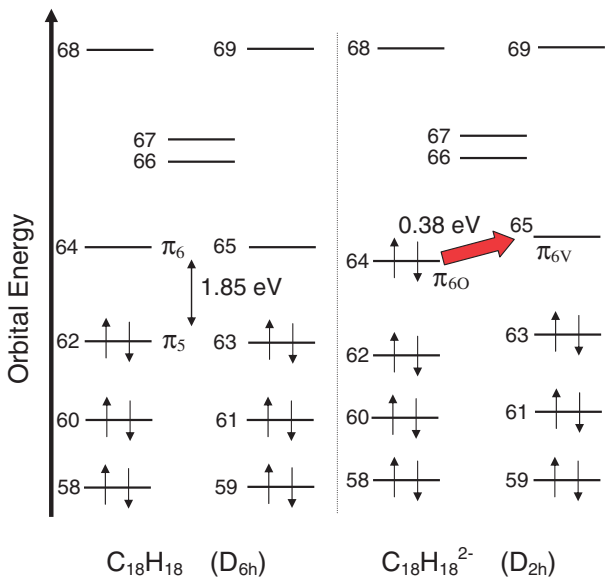

Figure 3. Orbital energies of $C_{18}H_{18}$ and $C_{18}H_{18}^{2-}$ and electronic transitions which mainly contribute into σ(*para*).

is an aromatic compound and the latter is an antiaromatic compound. In the Pople model, the ring current of an antiaromatic molecule is in reverse direction from that of an aromatic molecule. Therefore, $C_{18}H_{18}^{2-}$ turned out to be an antiaromatic molecule.

In order to analyze the above results, we decomposed ^{1}H magnetic shielding constants of $C_{18}H_{18}$ and $C_{18}H_{18}^{2-}$ into σ(*dia*) and σ(*para*) in Table 3. The values of σ(*dia*) of H(out) and H(in) slightly change between $C_{18}H_{18}$ and $C_{18}H_{18}^{2-}$, while σ(*para*) essentially contributes σ(*total*). An analysis for σ(*para*) is required in further discussions. Figure 3 shows electron configurations of $C_{18}H_{18}$ and $C_{18}H_{18}^{2-}$. In $C_{18}H_{18}$, the degenerate π_5 orbitals are the HOMOs and the π_6 orbitals are the LUMOs. In $C_{18}H_{18}^{2-}$, by adding two electrons, the molecular structure is distorted from D_{6h} to D_{2h}. The π_{6O} orbital is the HOMO and the π_{6V} orbital is the LUMO. Equation 4 suggests that low-lying magnetically allowed transitions mainly contribute to σ(*para*), and indeed the HOMO–LUMO transitions shown in Figure 3 contribute 58% and 99% of σ(*para*) in $C_{18}H_{18}$ and $C_{18}H_{18}^{2-}$, respectively. The energy gap between the π_5 and π_6 orbitals of $C_{18}H_{18}$ is 0.068 hartree = 1.85 eV, while that between the π_{6O} and π_{6V} orbitals of $C_{18}H_{18}^{2-}$ is 0.014 hartree = 0.38 eV. Therefore, the magnitude of σ(*para*) for $C_{18}H_{18}^{2-}$ is larger than that for $C_{18}H_{18}$.

We further decomposed the ^{1}H magnetic shielding constants of $C_{18}H_{18}$ and $C_{18}H_{18}^{2-}$ into their *xx*, *yy*, and *zz* components, and the results are listed in Table 4. The coordinate axes are shown in Figure 4. As we discussed above, σ(*para*) is the origin of the difference in ^{1}H magnetic shielding constants between $C_{18}H_{18}$ and $C_{18}H_{18}^{2-}$. Especially, the *zz* components of H(in) mainly contribute to the difference of ^{1}H magnetic shielding constants. The values of $\sigma(para)_{zz}$ for $C_{18}H_{18}$ and $C_{18}H_{18}^{2-}$ were +37.29 and −63.87 ppm, respectively. We can explain this tendency as follows. Assuming that H(in) is almost on the center of the ring, the $\sigma(para)_{zz}$ of H(in) for $C_{18}H_{18}$ and $C_{18}H_{18}^{2-}$ are approximately expressed by eqs 8 and 9, respectively.

$$\sigma(para)_{zz} \approx \frac{e^2\mu_0}{2m_e^2}\sum_{O,V}\frac{\langle\pi_O|\hat{L}_z|\pi_V\rangle\langle\pi_V|r_N^{-3}\hat{L}_{Nz}|\pi_O\rangle}{E_O - E_V}$$
$$= \frac{e^2\mu_0}{2m_e^2}\frac{\langle\pi_5|\hat{L}_z|\pi_6\rangle\langle\pi_6|r_N^{-3}\hat{L}_{Nz}|\pi_5\rangle}{E_5 - E_6} + \cdots$$
$$\approx 0 \quad (E_5 \ll E_6) \tag{8}$$

Table 4. Decomposition of the ^{1}H Magnetic Shielding Constants into Their *xx*, *yy*, and *zz* Components (ppm)

	Number of π-electron			dia	para	total
$C_{18}H_{18}$	18	H(out)	σ_{xx}	29.36	−0.22	29.14
			σ_{yy}	42.49	−17.73	24.76
			σ_{zz}	17.30	−10.61	6.69
			σ_{iso}	29.71	−9.52	20.19
$C_{18}H_{18}$	18	H(in)	σ_{xx}	35.23	−4.79	30.44
			σ_{yy}	36.58	−19.13	17.45
			σ_{zz}	45.15	37.29	82.44
			σ_{iso}	38.99	4.46	43.45
$C_{18}H_{18}^{2-}$	20	H(out)	σ_{xx}	21.83	14.52	36.35
			σ_{yy}	31.94	−0.23	31.71
			σ_{zz}	43.41	−13.41	30.00
			σ_{iso}	32.39	0.29	32.68
$C_{18}H_{18}^{2-}$	20	H(in)	σ_{xx}	35.07	−5.00	30.07
			σ_{yy}	39.75	−19.29	20.46
			σ_{zz}	37.05	−63.87	−26.82
			σ_{iso}	37.29	−29.39	7.90

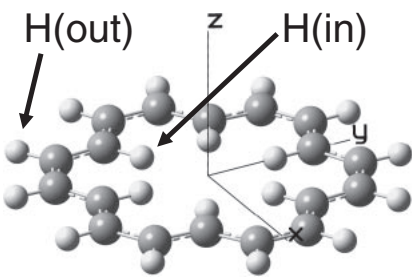

Figure 4. Coordinate axes of $C_{18}H_{18}$ and $C_{18}H_{18}^{2-}$.

$$\sigma(para)_{zz} \approx \frac{e^2\mu_0}{2{m_e}^2}\sum_{O,V}\frac{\langle\pi_O|\hat{L}_z|\pi_V\rangle\langle\pi_V|{r_N}^{-3}\hat{L}_{Nz}|\pi_O\rangle}{E_O - E_V}$$
$$\approx \frac{e^2\mu_0}{2{m_e}^2}\frac{\langle\pi_{6O}|\hat{L}_z|\pi_{6V}\rangle\langle\pi_{6V}|{r_N}^{-3}\hat{L}_{Nz}|\pi_{6O}\rangle}{E_{6O} - E_{6V}}$$
$$< 0 \quad (E_{6O} \approx E_{6V}) \tag{9}$$

where π_O and π_V are occupied and virtual π orbitals, respectively, and refer to Figure 3 for the definition of π_5, π_6, π_{6O}, and π_{6V} orbitals. According to these formulae, it is expected that $\sigma(para)_{zz}$ for $C_{18}H_{18} > \sigma(para)_{zz}$ for $C_{18}H_{18}^{2-}$, and this fact affects the difference of $\sigma(para)$ between $C_{18}H_{18}$ and $C_{18}H_{18}^{2-}$. This is an essential difference between $4n$ and $(4n + 2)$ systems.

[18]Annulene Analogues. Table 3 also shows the ^{1}H magnetic shielding constants of some analogue molecules from [18]annulene, such as $C_{16}H_{18}$, $C_{18}H_{20}$, and two modified systems, $C_{18}H_{20} + CH_3^-$ and $C_{16}H_{18} + H_2C{=}CH_2$. Figure 5 shows the molecular structure of $C_{16}H_{18}$ which was made by removing a C_2H_4 fragment from the optimized $C_{18}H_{18}$ and adding two hydrogen atoms so that all the C–H bond lengths and C–C–H angles are the same in the molecule. As shown in Figure 6, $C_{18}H_{20}$ is constructed by breaking a C–C σ-bond of the optimized [18]annulene and distorting the ring form helically from the planar structure as the two terminal π-orbitals can interact weakly with each other, and then adding two hydrogen atoms to the terminal carbons in the same way as $C_{16}H_{18}$. We call this $C_{18}H_{20}$ a quasi-Möbius-type molecule. The R value in Figure 6 is the horizontal distance between the terminal CH_2 planes. We calculated ^{1}H shielding constants for $R = 1.5$, 2.0, and 3.0 Å. Figure 7 shows a modified quasi-Möbius-type $C_{18}H_{20}$ ($R = 3.0$ Å) into which an optimized methyl anion (CH_3^-) is inserted. Figure 8 shows another quasi-Möbius-type system $C_{16}H_{18} + H_2C{=}CH_2$, where the ethylene molecule is optimized by B3LYP/6-311G(d,p) similarly.

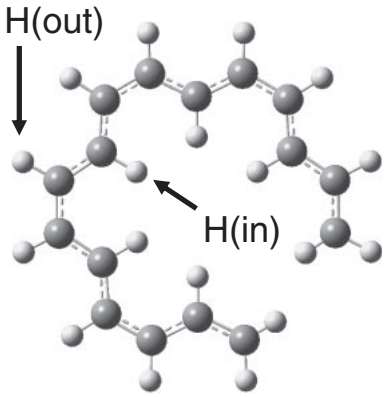

Figure 5. Molecular structure of $C_{16}H_{18}$.

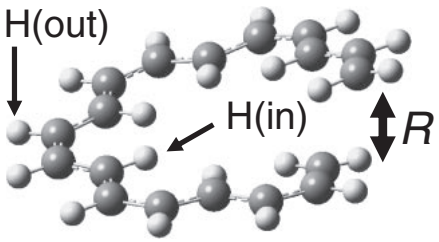

Figure 6. Molecular structure of quasi-Möbius-type $C_{18}H_{20}$ ($R = 1.5$ Å).

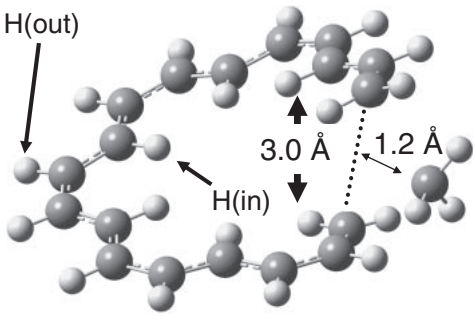

Figure 7. Molecular structure of quasi-Möbius-type $C_{18}H_{20}$. A methyl anion CH_3^- is inserted between the terminal π-orbitals.

In open-chain $C_{16}H_{18}$, the $\sigma(total)$ values of H(out) and H(in) were close to each other (H(out) = 25.74 ppm, H(in) = 22.63 ppm). The aromaticity of open-chain $C_{16}H_{16}$ completely vanished because of cutting the aromatic ring. In quasi-Möbius-type $C_{18}H_{20}$ ($R = 1.5$ Å), a magnetic shielding contrary to that of $C_{18}H_{18}$ is generated. They were 29.82 and 6.90 ppm for H(out) and H(in), respectively. This trend is similar to $C_{18}H_{18}^{2-}$ that has an antiaromatic character in spite

that $C_{18}H_{20}$ has $(4n+2)\pi$-electrons similarly to aromatic $C_{18}H_{18}$. The HOMOs of $C_{18}H_{18}$ and $C_{18}H_{20}$ ($R = 1.5$ Å) are shown in Figures 9 and 10, respectively. Both orbitals have 4 nodes because of the same π-electron numbers. However, the positions of the nodes are quite different, reflecting their aromaticity. Figure 10 show that when one cuts an in-phase π-bond of the aromatic $C_{18}H_{18}$ and makes the helical $C_{18}H_{20}$ ($R = 1.5$ Å), two π-orbitals on the terminal carbons of the helical $C_{18}H_{20}$ can interact out-of-phase with each other. This situation is similar to the case of aromatic and Möbius ring molecules, and therefore, we call this helical molecule quasi-Möbius-type. This similarity will be further discussed in the next paragraph. In $R = 3.0$ Å, the difference between H(out) and H(in) was small, indicating that the antiaromaticity of the quasi-Möbius-type $C_{18}H_{20}$ disappears in a long R region.

The differences among the $C_{18}H_{18}$ and helical $C_{18}H_{20}$ systems can be understood by the 18×18 Hückel secular equations as

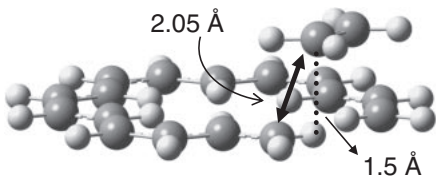

Figure 8. Molecular structure of quasi-Möbius-type $C_{18}H_{22}$ ($R = 1.5$ Å) which consists of $C_{16}H_{18}$ and $CH_2{=}CH_2$.

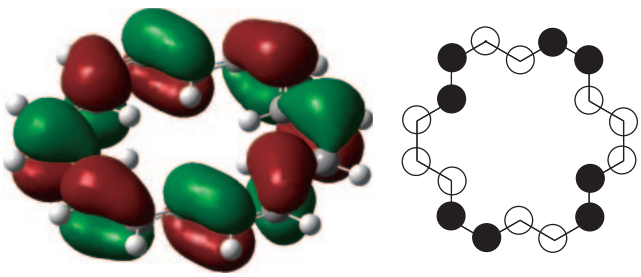

(a) (b)

Figure 9. Graphical and schematic pictures of the HOMO of [18]annulene ($C_{18}H_{18}$).

$$\begin{vmatrix} x & 1 & 0 & \cdots & \cdots & \cdots & 0 & 0 & 1 \\ 1 & x & 1 & \ddots & \ddots & \ddots & 0 & 0 & 0 \\ 0 & 1 & x & \ddots & \ddots & \ddots & 0 & 0 & 0 \\ \vdots & \ddots & \ddots & \ddots & \ddots & \ddots & \ddots & \ddots & \vdots \\ \vdots & \ddots & \ddots & \ddots & \ddots & \ddots & \ddots & \ddots & \vdots \\ \vdots & \ddots & \ddots & \ddots & \ddots & \ddots & \ddots & \ddots & \vdots \\ 0 & 0 & 0 & \ddots & \ddots & \ddots & x & 1 & 0 \\ 0 & 0 & 0 & \ddots & \ddots & \ddots & 1 & x & 1 \\ 1 & 0 & 0 & \cdots & \cdots & \cdots & 0 & 1 & x \end{vmatrix} = 0 \qquad (10)$$

and

$$\begin{vmatrix} x & 1 & 0 & \cdots & \cdots & \cdots & 0 & 0 & -\theta \\ 1 & x & 1 & \ddots & \ddots & \ddots & 0 & 0 & 0 \\ 0 & 1 & x & \ddots & \ddots & \ddots & 0 & 0 & 0 \\ \vdots & \ddots & \ddots & \ddots & \ddots & \ddots & \ddots & \ddots & \vdots \\ \vdots & \ddots & \ddots & \ddots & \ddots & \ddots & \ddots & \ddots & \vdots \\ \vdots & \ddots & \ddots & \ddots & \ddots & \ddots & \ddots & \ddots & \vdots \\ 0 & 0 & 0 & \ddots & \ddots & \ddots & x & 1 & 0 \\ 0 & 0 & 0 & \ddots & \ddots & \ddots & 1 & x & 1 \\ -\theta & 0 & 0 & \cdots & \cdots & \cdots & 0 & 1 & x \end{vmatrix} = 0 \qquad (11)$$

for $C_{18}H_{18}$ and $C_{18}H_{20}$, respectively. The Hückel interaction energy between the terminal π-orbitals is assumed to be $\theta\beta$ $(0 < \theta < 1)$ where β is the Hückel resonance integral. In case of $\theta = 1$, eq 9 is equivalent to the Möbius-type Hückel secular equation, while this Hückel equation can be regarded as quasi-Möbius-type for $0 < \theta < 1$. The total interaction energy among the π-electrons of $C_{18}H_{18}$ is 23.04β and that of $C_{18}H_{20}$ ($R = 1.5$ Å) is 22.69β assuming $\theta = 1$. Therefore, $C_{18}H_{18}$ is expected to be more stable than $C_{18}H_{20}$ ($R = 1.5$ Å) in energy.

Furthermore, we inserted a methyl anion, CH_3^-, into the quasi-Möbius-type $C_{18}H_{20}$ ($R = 3.0$ Å). The shape of

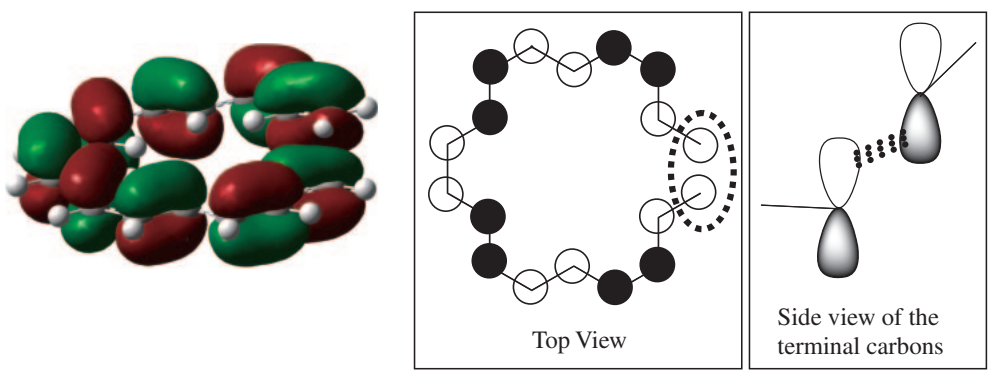

(a) (b)

Figure 10. Graphical and schematic pictures of the HOMO of quasi-Möbius-type $C_{18}H_{20}$ ($R = 1.5$ Å). When one cuts an in-phase π-bond of the aromatic $C_{18}H_{18}$ and makes the helical $C_{18}H_{20}$, two π-orbitals on the terminal carbons of the helical $C_{18}H_{20}$ can interact out-of-phase with each other, like a Möbius ring molecule.

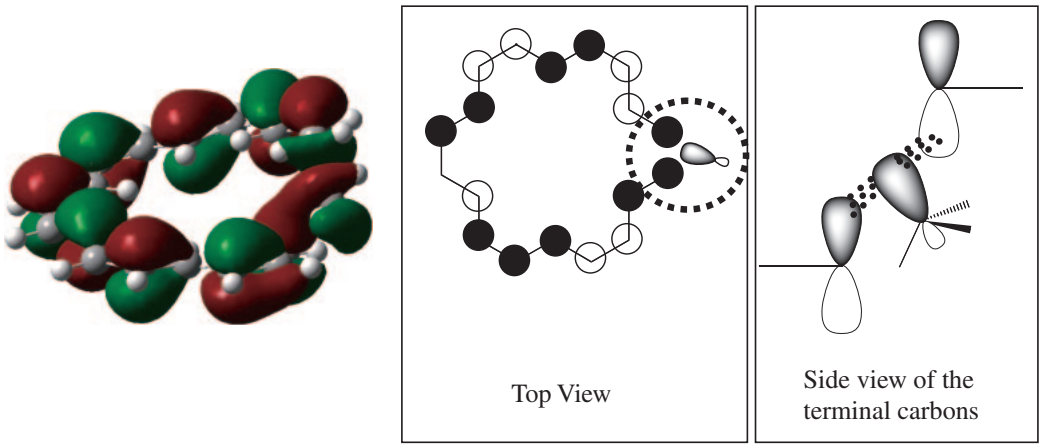

Figure 11. Graphical and schematic pictures of the HOMO of quasi-Möbius-type $C_{18}H_{20}$ ($R = 3.0$ Å) + CH_3^-.

the HOMO for $C_{18}H_{20} + CH_3^-$ in Figure 11 indicates that the sp^3 orbital of the CH_3^- interacts with the $2p_z$ orbitals (π orbitals) at the terminal carbons and we can regard this system as a "ring" again. The difference in the shielding constants between H(out) and H(in) becomes larger than the separated quasi-Möbius-type $C_{18}H_{20}$ ($R = 3.0$ Å); 25.43 and 30.77 ppm for H(out) and H(in), respectively. This indicates that this system can be regarded as aromatic contrastive to the antiaromatic $C_{18}H_{20}$ system. The 19×19 secular equations of $C_{18}H_{20} + CH_3^-$ can be expressed as

$$\begin{vmatrix} x & 1 & 0 & \cdots & \cdots & \cdots & 0 & 0 & -\theta \\ 1 & x & 1 & \ddots & \ddots & \ddots & 0 & 0 & 0 \\ 0 & 1 & x & \ddots & \ddots & \ddots & 0 & 0 & 0 \\ \vdots & \ddots & \ddots & \ddots & \ddots & \ddots & \ddots & \ddots & \vdots \\ \vdots & \ddots & \ddots & \ddots & \ddots & \ddots & \ddots & \ddots & \vdots \\ \vdots & \ddots & \ddots & \ddots & \ddots & \ddots & \ddots & \ddots & \vdots \\ 0 & 0 & 0 & \ddots & \ddots & \ddots & x & 1 & 0 \\ 0 & 0 & 0 & \ddots & \ddots & \ddots & 1 & x & \theta \\ -\theta & 0 & 0 & \cdots & \cdots & \cdots & 0 & \theta & x+\xi \end{vmatrix} = 0 \quad (12)$$

The definition of θ ($0 < \theta < 1$) is the same as that in eq 11, and ξ is added to describe the sp^3 orbital. Assuming $\theta = 1$ and $\xi = 3$, the total π-electron interaction energy of $C_{18}H_{20} + CH_3^-$ is 28.86β. Comparing the interaction energies of $C_{18}H_{18}$, $C_{18}H_{20}$ ($R = 1.5$ Å), and $C_{18}H_{20} + CH_3^-$, it seems that $C_{18}H_{20} + CH_3^-$ has the largest stabilization by π electrons in the Hückel level.

We can propose another quasi-Möbius-type complex, $C_{16}H_{18} + H_2C{=}CH_2$, shown in Figure 8. The HOMO of $C_{16}H_{18} + H_2C{=}CH_2$ is shown in Figure 12. Similar to the previous system, $C_{16}H_{18}$ is not a ring molecule, whereas π-orbitals of the C_2H_4 interact with those of the $C_{16}H_{18}$ and make this system a ring. The 18×18 Hückel secular equation of this complex is given by

$$\begin{vmatrix} x & 1 & 0 & \cdots & \cdots & \cdots & 0 & 0 & \theta \\ 1 & x & 1 & \ddots & \ddots & \ddots & 0 & 0 & 0 \\ 0 & 1 & x & \ddots & \ddots & \ddots & 0 & 0 & 0 \\ \vdots & \ddots & \ddots & \ddots & \ddots & \ddots & \ddots & \ddots & \vdots \\ \vdots & \ddots & \ddots & \ddots & \ddots & \ddots & \ddots & \ddots & \vdots \\ \vdots & \ddots & \ddots & \ddots & \ddots & \ddots & \ddots & \ddots & \vdots \\ 0 & 0 & 0 & \ddots & \ddots & \ddots & x & \theta & 0 \\ 0 & 0 & 0 & \ddots & \ddots & \ddots & \theta & x & 1 \\ \theta & 0 & 0 & \cdots & \cdots & \cdots & 0 & 1 & x \end{vmatrix} = 0 \quad (13)$$

Assuming $\theta = 1$, this secular equation is identical to eq 10. The magnetic shielding tensors are shown in Table 3 and are 23.94 and 30.10 ppm for H(out) and H(in), respectively. Since H(in) is shielded, we can regard this system as aromatic. The difference between H(out) and H(in), i.e., the aromaticity of this system, is stronger than that of $C_{18}H_{20} + CH_3^-$.

The results of proton shielding constants are illustrated in Figure 13 for the ring and Möbius-ring molecular systems we studied. The magnetic shieldings become completely opposite between $C_{18}H_{18}$ and $C_{18}H_{18}^{2-}$. In $C_{18}H_{18}$, the H(in) is shielded (upfield shift) and the H(out) is deshielded (downfield shift), whereas the H(in) is deshielded (downfield shift) and the H(out) is shielded (upfield shift) in $C_{18}H_{18}^{2-}$. For $C_{16}H_{18}$, differences between the H(out) and the H(in) become almost extinct because of the ring breaking. A quasi-Möbius-type analogue of [18]annulene, $C_{18}H_{20}$ ($R = 1.5$ Å), shows the antiaromatic magnetic shielding similar to $C_{18}H_{18}^{2-}$, i.e., the H(in) is deshielded (downfield shift) and the H(out) is shielded (upfield shift). When we insert CH_3^- into the quasi-Möbius-type $C_{18}H_{20}$, the aromaticity is recovered, namely, the H(in) and the H(out) are shielded and deshielded, respectively. The $C_{16}H_{18} + H_2C{=}CH_2$ system has a Hückel secular equation similar to the aromatic $C_{18}H_{18}$, and therefore, it also shows the aromatic magnetic shielding as well as $C_{18}H_{18}$.

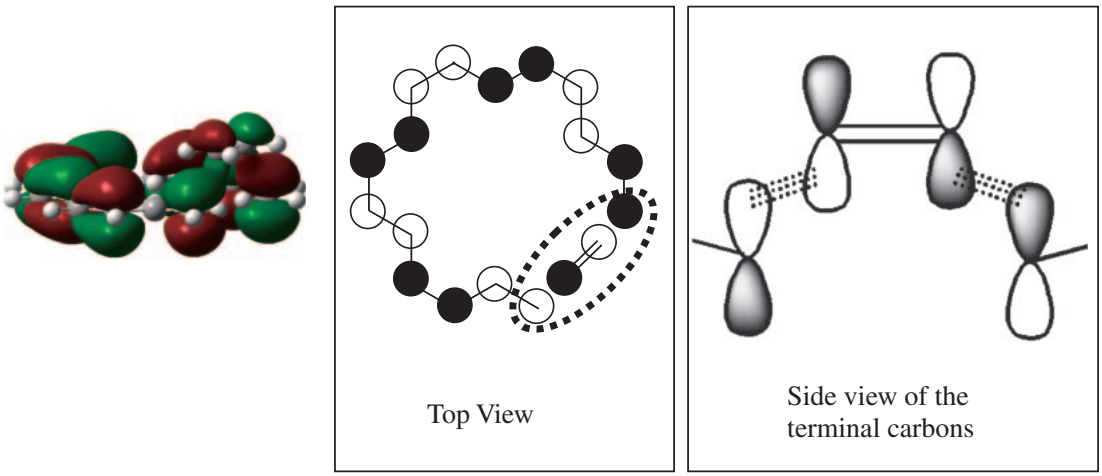

Figure 12. Graphical and schematic pictures of the HOMO of quasi-Möbius-type $C_{16}H_{18} + H_2C{=}CH_2$ ($R = 3.0$ Å).

Table 5. NICS(0) Values of $C_{18}H_{18}$, $C_{18}H_{18}^{2-}$, $C_{16}H_{18}$, Quasi-Möbius-Type $C_{18}H_{20}$ ($R = 1.5$, 2.0, and 3.0 Å), Quasi-Möbius-Type $C_{18}H_{20} + CH_3^-$, and $C_{16}H_{18} + H_2C{=}CH_2$ (ppm)

Molecule	Number of π-electron	σ of the ring center			NICS(0)
		$\sigma(dia)$	$\sigma(para)$	$\sigma(total)$	
$C_{18}H_{18}$	18	7.42	7.84	15.26	−15.26
$C_{18}H_{18}^{2-}$	20	4.69	−19.20	−14.51	14.51
$C_{16}H_{18}$	16	6.45	−9.21	−2.76	2.76
Möbius-type $C_{18}H_{20}$ ($R = 1.5$ Å)	18	7.64	−23.47	−15.83	15.83
Möbius-type $C_{18}H_{20}$ ($R = 2.0$ Å)	18	6.97	−15.76	−8.79	8.79
Möbius-type $C_{18}H_{20}$ ($R = 3.0$ Å)	18	8.93	−12.75	−3.82	3.82
Möbius-type $C_{18}H_{20} + CH_3^-$	20	6.26	−1.62	4.64	−4.64
$C_{16}H_{18} + H_2C{=}CH_2$	18	5.40	−2.12	3.28	−3.28

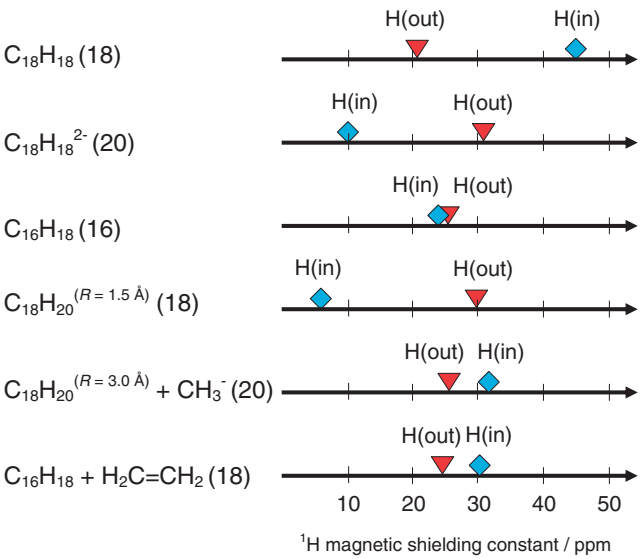

Figure 13. Magnetic shielding constants (ppm) of proton in various molecules. The values in the parentheses are numbers of π-electrons for each system.

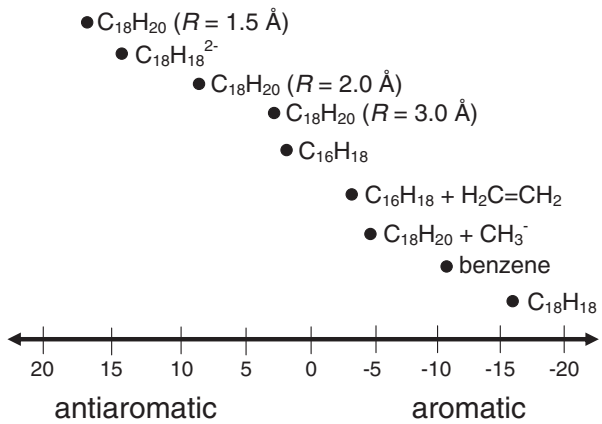

Figure 14. Calculated NICS(0) values (ppm) of $C_{18}H_{20}$ and its analogues together with benzene (ppm).

Table 5 shows NICS(0) values of $C_{18}H_{18}$, $C_{18}H_{18}^{2-}$, $C_{16}H_{18}$, quasi-Möbius-type $C_{18}H_{20}$ ($R = 1.5$, 2.0, and 3.0 Å), $C_{18}H_{20} + CH_3^-$, and $C_{18}H_{20} + H_2C{=}CH_2$, and their trends are illustrated in Figure 14. The NICS(0) value of benzene is also shown in this figure as a reference and was calculated to be −10.48 ppm at the present level of calculation method. Negative and positive NICS(0) values represents aromatic and antiaromatic characters, respectively. The NICS(0) of $C_{18}H_{18}$ is a large negative value (−15.26 ppm), indicating that this system has strong aromaticity. In contrast, the NICS(0) of $C_{18}H_{18}^{2-}$ is a large positive value (14.51 ppm), and therefore, it exhibits strong

antiaromaticity. A quasi-Möbius-type $C_{18}H_{20}$ ($R = 1.5$ Å) has a large positive NICS(0) value (15.83 ppm), i.e., a strong antiaromatic character. When a CH_3^- anion is inserted into the quasi-Möbius-type $C_{18}H_{20}$ ($R = 3.0$ Å), the NICS(0) value becomes negative, indicating that $C_{18}H_{20}$ ($R = 3.0$ Å) + CH_3^- shows weak aromaticity. When an ethylene molecule is put on $C_{16}H_{18}$, the NICS(0) becomes −3.28 ppm, which corresponds to a weak aromatic character. These results are almost consistent with the results of the shielding constants for H(in) and H(out) summarized in Table 3 and Figure 13. The NICS(0) values can be also decomposed into their $\sigma(dia)$ and $\sigma(para)$ components. The $\sigma(para)$ of $C_{18}H_{18}$ and $C_{18}H_{18}^{2-}$ is 7.84 and −19.20 ppm, respectively. The difference of the $\sigma(para)$ is larger than the $\sigma(dia)$, and the $\sigma(para)$ controls the NICS(0) values. Also in quasi-Möbius-type $C_{18}H_{20}$, when we gradually elongate R, the $\sigma(para)$ changes greatly (from −23.47 to −12.75 ppm), whereas the $\sigma(dia)$ does not change very much. The $\sigma(para)$ values of the NICS(0) for $C_{18}H_{20} + CH_3^-$ and $C_{16}H_{18} + H_2C{=}CH_2$ are very small, indicating that the ring current may be weak in these systems. This is consistent with the fact that these systems have weak aromaticity, i.e., small differences in the proton shielding constants between H(out) and H(in).

Conclusion

We carried out a series of the ab initio quantum-chemical calculations of $C_{18}H_{18}$ and its quasi-Möbius-type analogues from $C_{18}H_{18}$ and discussed the calculated nuclear magnetic shielding tensors, chemical shifts, and NICS(0). We also discussed aromaticity or antiaromaticity of these molecules based on the results of their magnetic properties.

(1) The experimental trends of the ^{1}H NMR chemical shifts for $C_{18}H_{18}$ (18π-electrons) and $C_{18}H_{18}^{2-}$ (20π-electrons) were reproduced by the present calculations. The former molecule exhibited aromatic character and the latter was antiaromatic. The decomposition of the magnetic shielding tensors reasonably explained the difference between the aromatic and antiaromatic molecules.

(2) A concept of quasi-Möbius-type molecules was presented. In $C_{18}H_{20}$, which is generated from $C_{18}H_{18}$ (18π-electrons) and $C_{18}H_{20} + CH_3^-$ (20π-electrons), the conventional Möbius rule still worked well. The quasi-Möbius-type $C_{18}H_{20}$ had antiaromatic character due to the weak interaction between the terminal $2p_z$ orbitals. The $C_{18}H_{20} + CH_3^-$ complex was suggested to be an aromatic Möbius-type system with the $4n\pi$-electrons.

(3) We carried out the NICS(0) calculations. $C_{18}H_{18}$ has a negative NICS(0), i.e., aromatic character. Quasi-Möbius-type $C_{18}H_{20}$ has an antiaromatic character and the systems $C_{18}H_{20} + CH_3^-$ and $C_{16}H_{18} + H_2C{=}CH_2$ are aromatic judging from the NICS(0) values. These results are consistent with the ^{1}H NMR data.

This work was supported by Japan Science and Technology (JST) Agency.

References

1 P. v. R. Schleyer, *Chem. Rev.* **2005**, *105*, 3433.
2 M. Jones, Jr., *Organic Chemistry*, 3rd ed., W. W. Norton & Co. Inc., **2005**.
3 E. Hückel, *Z. Phys. A: Hadrons Nucl.* **1931**, *70*, 204.
4 E. Hückel, *Z. Phys. A: Hadrons Nucl.* **1931**, *72*, 310.
5 E. Hückel, *Z. Phys. A: Hadrons Nucl.* **1932**, *76*, 628.
6 L. Pauling, *J. Chem. Phys.* **1936**, *4*, 673.
7 N. Jux, *Angew. Chem., Int. Ed.* **2008**, *47*, 2543.
8 H. S. Rzepa, *Chem. Rev.* **2005**, *105*, 3697.
9 Z. S. Yoon, A. Osuka, D. Kim, *Nat. Chem.* **2009**, *1*, 113.
10 E. Heilbronner, *Tetrahedron Lett.* **1964**, *5*, 1923.
11 N. Mizoguchi, *Chem. Phys. Lett.* **1987**, *134*, 371.
12 N. Mizoguchi, *J. Mol. Struct.: THEOCHEM* **1988**, *181*, 245.
13 D. Ajami, O. Oeckler, A. Simon, R. Herges, *Nature* **2003**, *426*, 819.
14 M. Stępień, L. Latos-Grażyński, N. Sprutta, P. Chwalisz, L. Szterenberg, *Angew. Chem., Int. Ed.* **2007**, *46*, 7869.
15 Y. Tanaka, S. Saito, S. Mori, N. Aratani, H. Shinokubo, N. Shibata, Y. Higuchi, Z. S. Yoon, K. S. Kim, S. B. Noh, J. K. Park, D. Kim, A. Osuka, *Angew. Chem., Int. Ed.* **2008**, *47*, 681.
16 S. Tokuji, J.-Y. Shin, K. S. Kim, J. M. Lim, K. Youfu, S. Saito, D. Kim, A. Osuka, *J. Am. Chem. Soc.* **2009**, *131*, 7240.
17 J. M. Lim, J.-Y. Shin, Y. Tanaka, S. Saito, A. Osuka, D. Kim, *J. Am. Chem. Soc.* **2010**, *132*, 3105.
18 M. Stępień, B. Szyszko, L. Latos-Grażyński, *J. Am. Chem. Soc.* **2010**, *132*, 3140.
19 C. Castro, C. M. Isborn, W. L. Karney, M. Mauksch, P. v. R. Schleyer, *Org. Lett.* **2002**, *4*, 3431.
20 P. M. Warner, *J. Org. Chem.* **2006**, *71*, 9271.
21 T. Heine, R. Islas, G. Merino, *J. Comput. Chem.* **2007**, *28*, 302.
22 E.-K. Mucke, F. Köhler, R. Herges, *Org. Lett.* **2010**, *12*, 1708.
23 S. Taubert, D. Sundholm, F. Pichierri, *J. Org. Chem.* **2009**, *74*, 6495.
24 H. Fliegl, D. Sundholm, S. Taubert, J. Juselius, W. Klopper, *J. Phys. Chem. A* **2009**, *113*, 8668.
25 K. Lonsdale, *Proc. R. Soc. London, Ser. A* **1937**, *159*, 149.
26 F. London, *C. R. Acad. Sci., Paris* **1937**, *28*, 205.
27 F. London, *J. Phys. Radium* **1937**, *8*, 397.
28 F. London, *J. Chem. Phys.* **1937**, *5*, 837.
29 J. A. Pople, W. G. Schneider, H. J. Bernstein, *High-Resolution Nuclear Magnetic Resonance*, McGraw-Hill, New York, **1959**.
30 H. Günther, *NMR Spectroscopy: Basic Principles, Concepts, and Applications in Chemistry*, 2nd ed., Wiley, New York, **1998**.
31 R. M. Silverstein, G. C. Bassler, T. C. Morill, *Spectrometric Identification of Organic Compounds*, 5th ed., Wiley & Sons, New York, **1991**.
32 C. S. Wannere, P. v. R. Schleyer, *Org. Lett.* **2003**, *5*, 605.
33 P. v. R. Schleyer, C. Maerker, A. Dransfeld, H. Jiao, N. J. R. E. Hommes, *J. Am. Chem. Soc.* **1996**, *118*, 6317.
34 Z. Chen, C. S. Wannere, C. Corminboeuf, R. Puchta, P. v. R. Schleyer, *Chem. Rev.* **2005**, *105*, 3842.
35 F. Sondheimer, R. Wolovsky, Y. Amiel, *J. Am. Chem. Soc.* **1962**, *84*, 274.
36 C. Weiss, Jr., M. Gouterman, *J. Chem. Phys.* **1965**, *43*, 1838.
37 a) R. C. Haddon, *Chem. Phys. Lett.* **1980**, *70*, 210. b) R. C. Haddon, K. Raghavachari, *J. Am. Chem. Soc.* **1985**, *107*, 289.
38 K. Jug, E. Fasold, *J. Am. Chem. Soc.* **1987**, *109*, 2263.
39 K. K. Baldridge, J. S. Siegel, *Angew. Chem., Int. Ed. Engl.* **1997**, *36*, 745.

40 N. F. Ramsey, *Phys. Rev.* **1950**, *77*, 567.
41 N. F. Ramsey, *Phys. Rev.* **1950**, *78*, 699.
42 N. F. Ramsey, *Phys. Rev.* **1951**, *83*, 540.
43 N. F. Ramsey, *Phys. Rev.* **1952**, *86*, 243.
44 H. Nakatsuji, K. Kanda, K. Endo, T. Yonezawa, *J. Am. Chem. Soc.* **1984**, *106*, 4653.
45 K. Kanda, H. Nakatsuji, T. Yonezawa, *J. Am. Chem. Soc.* **1984**, *106*, 5888.
46 R. Ditchfield, *Mol. Phys.* **1974**, *27*, 789.
47 M. J. Frisch, G. W. Trucks, H. B. Schlegel, G. E. Scuseria, M. A. Robb, J. R. Cheeseman, J. A. Montgomery, Jr., T. Vreven, K. N. Kudin, J. C. Burant, J. M. Millam, S. S. Iyengar, J. Tomasi, V. Barone, B. Mennucci, M. Cossi, G. Scalmani, N. Rega, G. A. Petersson, H. Nakatsuji, M. Hada, M. Ehara, K. Toyota, R. Fukuda, J. Hasegawa, M. Ishida, T. Nakajima, Y. Honda, O. Kitao, H. Nakai, M. Klene, X. Li, J. E. Knox, H. P. Hratchian, J. B. Cross, C. Adamo, J. Jaramillo, R. Gomperts, R. E. Stratmann, O. Yazyev, A. J. Austin, R. Cammi, C. Pomelli, J. W. Ochterski, P. Y. Ayala, K. Morokuma, G. A. Voth, P. Salvador, J. J. Dannenberg, V. G. Zakrzewski, S. Dapprich, A. D. Daniels, M. C. Strain, O. Farkas, D. K. Malick, A. D. Rabuck, K. Raghavachari, J. B. Foresman, J. V. Ortiz, Q. Cui, A. G. Baboul, S. Clifford, J. Cioslowski, B. B. Stefanov, G. Liu, A. Liashenko, P. Piskorz, I. Komaromi, R. L. Martin, D. J. Fox, T. Keith, M. A. Al-Laham, C. Y. Peng, A. Nanayakkara, M. Challacombe, P. M. W. Gill, B. Johnson, W. Chen, M. W. Wong, C. Gonzalez, J. A. Pople, *Gaussian 03 (Revision B.01)*, Gaussian, Inc., Pittsburgh PA, **2003**.
48 SDBSWeb: http://riodb01.ibase.aist.go.jp/sdbs/ (National Institute of Advanced Industrial Science and Technology, 2009/10).
49 R. G. Parr, W. Yang, *Density-Functional Theory of Atoms and Molecules*, Oxford Univ. Press, **1989**.
50 J. Bregman, F. L. Hirshfeld, D. Rabinovich, G. M. J. Schmidt, *Acta Crystallogr.* **1965**, *19*, 227.
51 F. L. Hirshfeld, D. Rabinovich, *Acta Crystallogr.* **1965**, *19*, 235.
52 L. M. Jackman, F. Sondheimer, Y. Amiel, D. A. Ben-Efraim, Y. Gaoni, R. Wolovsky, A. A. Bothner-By, *J. Am. Chem. Soc.* **1962**, *84*, 4307.
53 F. Sondheimer, *Acc. Chem. Res.* **1972**, *5*, 81.
54 J. F. M. Oth, E. P. Woo, F. Sondheimer, *J. Am. Chem. Soc.* **1973**, *95*, 7337.